Application of Scanning Electron Microscopy to X-ray Analysis of Frozen-hydrated Sections III. Elemental Content of Cells in the Rat Renal Papillary Tip

RUTH ELLEN BULGER, REINIER BEEUWKES III, and ALBERT J. SAUBERMANN
Department of Pathology and Laboratory Medicine, University of Texas Medical School at Houston, Houston, Texas 77025; Department of Physiology, Harvard Medical School, Boston, Massachusetts 02215; and Department of Anaesthesia Harvard Medical School at Beth Israel Hospital and C. Dana Research Institute, Boston, Massachusetts 02215

ABSTRACT The electrolyte and water content of cellular and interstitial compartments in the renal papilla of the rat was determined by x-ray microanalysis of frozen-hydrated tissue sections. Papillae from rats on ad libitum water were rapidly frozen in a slush of Freon 12, and sectioned in a cryomicrotome at −30 to −40°C. Frozen 0.5-μm sections were mounted on carbon-coated nylon film over a Be grid, transferred cold to the scanning microscope, and maintained at −175°C during analysis. The scanning transmission mode was used for imaging. Structural preservation was of good quality and allowed identification of tissue compartments. Tissue mass (solutes + water) was determined by continuum radiation from regions of interest. After drying in the SEM, elemental composition of morphologically defined compartments (solutes) was determined by analysis of specific x-rays, and total dry mass by continuum. Na, K, Cl, and H_2O contents in collecting-duct cells (CDC), papillary epithelial cells (PEC), and interstitial cells (IC) and space were measured. Cells had lower water content (mean 58.7%) than interstitium (77.5%). Intracellular K concentrations (millimoles per kilogram wet weight) were unremarkable (79–156 mm/kg wet weight); P was markedly higher in cells than in interstitium. S was the same in all compartments. Intracellular Na levels were extremely high (CDC, 344 ± 127 SD mm/kg wet weight; PEC, 287 ± 105; IC, 898 ± 194). Mean interstitial Na was 590 ± 119 mm/Kg wet weight. Cl values paralleled those for Na. If this Na is unbound, then these data suggest that renal papillary interstitial cells adapt to their hyperosmotic environment by a Na-uptake process.

Cells of the rat renal papilla are exposed to wide changes in the ionic and osmotic composition of their environment. The papillary epithelium of the rat is exposed to urine whose osmolality ranges from <100 to >3,000 mosmol/kg H_2O. Tubular and interstitial cells within the papilla live in the hypertonic environment associated with the urine-concentrating mechanism. Because few mammalian cell types are exposed to such environmental conditions, the mechanism by which these cells adapt to the high salt and urea content of their environment is of great interest to cell biologists. Schmidt-Nielsen (25) and Morgan (20), using in vitro centrifugation or incubation techniques, have reported that the Na content of papillary cells increases with increasing osmolality and reaches more than 400 mM. However, until recently no method existed for the definition of chemical composition of defined cell types within the papilla. The development of techniques for direct x-ray microanalysis of frozen-hydrated tissue sections (19, 22, 23) now makes such analysis possible.

MATERIALS AND METHODS

Six male Long-Evans rats (bred in our colony), weighing 125–200 g, were housed individually in metabolic cages for 2 d or more before the experiment. They were given Purina Rat Chow (0.29% Na, 0.46% K; Ralston Purina Co., St. Louis, Mo.) and water ad libitum. An overnight urine sample was collected and its osmolality determined. The kidneys were rapidly removed under pentobarbital anesthesia (50 mg/kg), and a small central wedge containing the renal papilla was immediately frozen by rapid immersion in Freon 12 at its melting point. The sample preparation techniques used in this study have been described and validated in detail (22, 23); hence, only an abstract of the techniques is given here. The frozen

THE JOURNAL OF CELL BIOLOGY · VOLUME 88 FEBRUARY 1981 274-280

papilla was mounted under liquid nitrogen in a precooled vise-type copper three-point holder. The tissue was sectioned on a Sorvall MT-2B microtome (DuPont Co., Sorvall Biomedical Div., Wilmington, Del.) provided with a cryochamber. The cooling system of the cryochamber was designed to surround the knife and specimen with a continuous flow of cold nitrogen gas. After a 20-min thermal equilibration period, sections (0.5 μm in thickness) were cut at −30 to −40°C with a steel razor blade and a specially designed glass antiroll plate. Frozen sections were transferred to a specimen holder within the cooled chamber by means of a cold eyelash attached to a wooden applicator stick. The specimen holder consisted of a 75-mesh beryllium grid mounted on a beryllium cylinder covered with a nylon film (~100-nm thick) and coated with a layer of carbon (10–200 nm).

The specimen holder was then transferred to a cold stage (−175°C) (22) in the vacuum column of an AMR 900 (AMRay Corp., Burlington, Mass.) scanning electron microscope, using a transfer device consisting of a cooled copper heat sink in a sealable Delrin cylinder. Spectra were obtained with a Kevex 5100 energy dispersive x-ray analysis system (Kevex Corp., Foster City, Calif.) with a 10-mm^2 155-eV resolution Si(Li) detector (working distance ~15 mm), x-ray mapping modules, and a PDP 11/03 computer (Digital Equipment Corp., Maynard, Mass.). A 30-keV accelerating voltage, 0.1-nA probe current (measured with a Faraday cup attached to the microscope cold stage), and 80-s live counting time were used for all measurements. The takeoff angle was 35°. An initial evaluation of each section was made by study of secondary and transmission electron images to determine its suitability for analysis. To aid in the selection of structures for analysis in hydrated sections where contrast in the STEM image was generally low, x-ray maps for phosphorus were collected on a storage oscilloscope. All regions analyzed were marked on photographs taken of the x-ray map and on the corresponding STEM images. Characteristic x-rays for each element were integrated over the following energy ranges: sodium, 0.96–1.12 keV; phosphorus, 1.92–2.08 keV; sulfur, 2.24–2.40 keV; chlorine, 2.52–2.68 keV; and potassium, 3.24–3.40 keV. Continuum radiation for measurement of tissue mass was integrated between 4.60 and 6.00 keV.

The Hall method was used for quantitation (16). This method employs the ratio of counts of characteristic x-rays to counts from the continuum (after correction for signals originating in the supporting film) as a measure proportional to mass fraction. Such ratios are expressed as R-values.

$$R\text{-value} = \frac{P_x - b_x}{W_T - W_E}, \quad (1)$$

where P_x = characteristic x-ray counts for element x, b_x = background counts under the characteristic peak, W_T = continuum ("white") counts in a selected region, and W_E = extraneous continuum counts.

The methods of calculation and the algorithms employed have been described in detail (22). Analyses were performed using both small raster scans over specific cell compartments selected on the basis of best morphological definition (9, 10) and large scans as a control for variation in section thickness. To define the water content within individual compartments, we analyzed selected regions in both hydrated and dried states. After analysis under hydrated conditions, sections were dried within the microscope by allowing the stage temperature to rise to −30°C. After drying was complete, the temperature of the cold stage was again lowered to −175°C and spectra were obtained under the same conditions employed previously. To calculate water content, the following formula was used:

$$\%\ water = \left[1 - \frac{Continuum_{dried}}{Continuum_{hydrated}}\right] \times 100\%. \quad (2)$$

Absolute mass fractions (concentrations) in millimoles per kilogram wet weight were calculated by the equations:

$$C_x = R_{x\,dry} S_x \text{ (mm/kg dry weight)} \quad (3)$$

and

$$C'_x = R_{x\,dry} S_x \left[\frac{100 - \%\ water}{100}\right] \text{ (mm/kg wet weight)}, \quad (4)$$

where S_x was a calibration factor defined by the slope of the best-fit regression line obtained in the analysis of known standards (22).

RESULTS

Image Quality

Cross sections of the entire papilla tip were obtained in the frozen-hydrated state. The frozen-hydrated sections were generally electron dense, with little cellular detail evident in the STEM image (Fig. 1). Because morphological compartments were difficult to define in the hydrated state,[1] x-ray mapping for phosphorus was useful in delineating the position of cells and tubules for analysis. After the sections were dried in the microscope and recooled for viewing, the following cellular and extracellular compartments could easily be identified: nucleus and cytoplasm of collecting-duct cells, papillary epithelial cells, and interstitial cells; interstitium, lumina of collecting ducts, capillaries, and thin limbs, and erythrocytes (Fig. 2). The reticulated pattern present within the tissue showed spaces that had presumably been occupied by ice crystals in the frozen-hydrated state. These spaces were largest in those cell compartments with the greatest hydration. The lumina of collecting ducts demonstrated various degrees of patency. The lumens of capillaries and thin limbs were always widely patent. Characteristic x-ray spectra were obtained from these compartments.

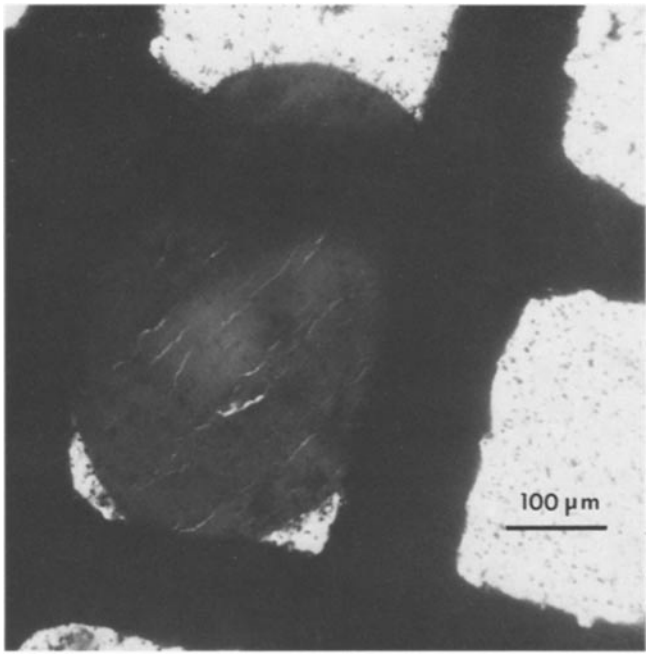

FIGURE 1 Scanning transmission micrograph of frozen-hydrated section of rat renal papilla. Because the electron density of frozen hydrated sections is nearly uniform, morphological detail is absent.

X-ray Analysis

Table I lists the calculated dry-weight mass fraction (R-values) for five elements measured in four major tissue compartments. The variance of these results was found to be much larger than expected from the variance inherent in the method (22). The additional variance arose primarily from differences among rats. Using calibration ratios previously defined by the analysis of known standards (22), we calculated the concentration in millimoles per kilogram dry weight (Eq. 3) for each compartment (Table II).

To express concentrations in terms of wet weight (Eq. 4), we computed the compartmental water content in five animals. The three cell types had similar water content (collecting-duct cells, 56.7 ± 5.6%; papillary epithelial cells, 59.5 ± 10.8%; and

[1] A detailed discussion of image quality in the scanning microscope as illustrated by kidney sections can be found in the first paper of this series (23).

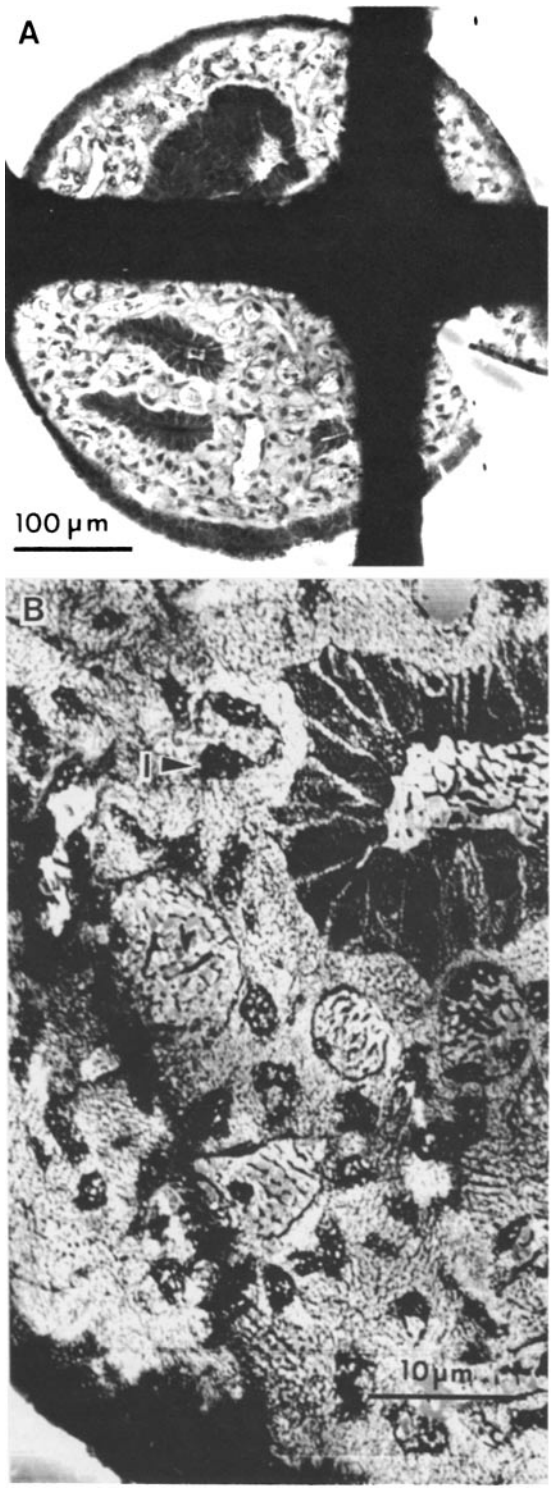

FIGURE 2 Scanning transmission micrographs of frozen-dried sections of rat renal papilla. *A*, low power view of complete cross section very near the papilla tip. The junction of a duct of Bellini with the papillary epithelium is seen in the upper left quadrant. *B*, high magnification. A collecting duct is seen at the upper right, and papillary epithelium at the lower left. The reticulated appearance of the tissue results from ice crystals formed during the initial freezing step. An interstitial cell is indicated (*I*).

interstitial cells, 59.9 ± 5.6%). The interstitium had a higher water content (77.5 ± 2.3%). The collecting-duct lumen water content was determined in one animal to be 82.8 ± 4.5%. Based on these water contents, the concentration of each measured element in millimoles per kilogram wet weight and grams per kilogram wet weight were computed for each compartment (Table II). No significant elemental differences were found in the wet weight or dry weight elemental composition of collecting-duct cells when compared with the papillary epithelial cells (Table III). The interstitial cells were significantly different from both papillary epithelial cells and collecting-duct cells, having much higher values for Na and Cl ($P < .001$) and lower values for K and P ($P < .01$). The interstitial cells were also significantly different from the interstitium in both percent water ($P < .001$) and in Na, K, Cl, and P wet weight fractions. No significant difference was seen in dry weight Na content. The P and K concentrations in the interstitium were significantly lower than in any cell compartment measured. Na concentrations were highest in interstitial cells, and lowest in collecting-duct and papillary epithelial cells. The differences in Na concentration between each of these cell types and that of the interstitium was highly significant.

These elemental concentration differences are seen in the x-ray spectra obtained from tissue compartments in both hydrated and dried sections. Fig. 3 shows typical spectra obtained from the following compartments in dried sections: (*a*) collecting-duct cytoplasm; (*b*) papillary epithelial cell cytoplasm; (*c*) interstitial cell cytoplasm; (*d*) interstitium; (*e*) collecting-duct lumen; and (*f*) capillary lumen.

DISCUSSION

Saubermann et al. (22, 23) have recently described a practical method for x-ray microanalysis of frozen-hydrated tissue sections in a scanning electron microscope fitted with an energy-dispersive x-ray detector. The first paper in this series (23) defined specimen-handling techniques that provide suitable cryosections for analysis, and a specimen support and transfer system that minimizes extraneous, interfering x-ray radiation and maximizes thermal conductivity so as to maintain hydration. The second paper (22) described the calculations used in this technique in detail, and validated the technique with respect to elemental displacement, ice-crystal size, and melting during sectioning. In addition, the analysis of known standard solutions prepared in a manner similar to that of tissue sections provided the standard curves used for calculations in the present study. The advantages of this approach for studies of the renal papilla are many. The technique has the resolution necessary to define compartments under direct visual control; it uses frozen-hydrated sections that allow direct measurement of solutes in their aqueous matrix and that preserve luminal contents; it allows sequential measurements of the same cellular and extracellular compartments in both frozen-hydrated and frozen-dried sections, and thus gives a direct measure of compartment water content and elemental concentrations in the hydrated state. The goal of the present study was to define the intracellular composition that permits cells to survive in the hypertonic environment of the renal papilla.

The overall papillary osmotic gradient for solutes was determined long ago by the study of the melting points of luminal contents in frozen papillary slices (29, 30). Such studies measured only total solute content. Numerous later studies analyzing whole papillae or slices by various techniques have shown that osmolality and sodium, potassium, and urea concentrations increase from the corticomedullary junction to the papillary tip, and vary with the degree of urine concentration (1, 3–6, 12, 13, 15, 18, 21). Although these studies defined the chemical species present, they did not distinguish among tissue

TABLE I

Compartmental R-values (Mass Fractions) of Elements as Measured in Dried Sections (± SD)

	Measurements	Na	P	S	Cl	K
	n					
COLLECTING-DUCT CELLS						
Rat 1	7	.104 ± .031	.354 ± .045	.059 ± .010	.615 ± .120	.286 ± .065
Rat 2	4	.035 ± .012	.400 ± .067	.051 ± .011	.280 ± .050	.458 ± .094
Rat 3	6	.053 ± .016	.394 ± .038	.063 ± .015	.416 ± .083	.409 ± .065
Rat 4	5	.055 ± .030	.350 ± .078	.032 ± .010	.252 ± .111	.164 ± .036
Rat 5	3	.079 ± .012	.331 ± .052	.042 ± .008	.394 ± .044	.244 ± .035
Rat 6	11	.061 ± .020	.392 ± .038	.054 ± .010	.395 ± .073	.311 ± .038
Average		.065 ± .024	.370 ± .029	.050 ± .011	.392 ± .128	.312 ± .108
PAPILLARY EPITHELIAL CELLS						
Rat 1	5	.083 ± .011	.273 ± .045	.129 ± .042	.416 ± .064	.278 ± .033
Rat 2	7	.044 ± .026	.380 ± .039	.158 ± .006	.290 ± .136	.257 ± .026
Rat 3	6	.042 ± .011	.518 ± .055	.075 ± .009	.407 ± .051	.417 ± .058
Rat 4	5	.077 ± .027	.323 ± .050	.056 ± .011	.587 ± .254	.232 ± .033
Rat 5	3	.065 ± .027	.366 ± .046	.043 ± .011	.388 ± .107	.267 ± .009
Rat 6	7	.031 ± .005	.429 ± .035	.064 ± .020	.337 ± .025	.353 ± .021
Average		.057 ± .021	.382 ± .085	.071 ± .030	.404 ± .101	.301 ± .070
INTERSTITIAL CELLS						
Rat 1	4	.239 ± .041	.236 ± .067	.059 ± .014	1.236 ± .163	.190 ± .028
Rat 2	4	.160 ± .018	.217 ± .032	.052 ± .017	.863 ± .118	.172 ± .007
Rat 3	6	.174 ± .031	.295 ± .036	.063 ± .019	.998 ± .089	.205 ± .025
Rat 4	5	.180 ± .017	.242 ± .086	.035 ± .023	.901 ± .049	.105 ± .011
Rat 5	7	.204 ± .004	.173 ± .052	.034 ± .018	.833 ± .041	.165 ± .003
Rat 6	9	.125 ± .038	.206 ± .053	.047 ± .007	.713 ± .120	.173 ± .029
Average		.180 ± .039	.228 ± .041	.048 ± .012	.924 ± .179	.168 ± .034
INTERSTITIUM						
Rat 1	4	.247 ± .029	.176 ± .040	.061 ± .018	1.318 ± .251	.181 ± .021
Rat 2	4	.163 ± .016	.093 ± .041	.129 ± .011	.839 ± .088	.173 ± .018
Rat 3	6	.204 ± .109	.153 ± .052	.089 ± .032	1.154 ± .037	.180 ± .011
Rat 4	5	.197 ± .020	.078 ± .039	.065 ± .022	.847 ± .075	.095 ± .009
Rat 5	4	.175 ± .034	.070 ± .015	.121 ± .027	.652 ± .109	.169 ± .030
Rat 6	7	.271 ± .021	.088 ± .034	.075 ± .015	1.199 ± .083	.178 ± .029
Average		.209 ± .042	.110 ± .044	.090 ± .029	1.002 ± .259	.163 ± .033

All R-values are expressed as mean ± SD of *n* measurements made in the same compartment. Overnight urine osmolality in these rats was: *1*, 1,668; *2*, 1,267; *3*, 2,221; *4*, 2,091; *5*, 1,977; *6*, 1,513.

compartments. Micropuncture studies have provided measurements of concentration in some luminal and vascular compartments (7, 14, 17, 28). However, micropuncture techniques can study only fluids that are obtainable from the papillary surface.

Schmidt-Nielsen (25), using a centrifuge technique, was able to collect fluid separately from extracellular and cellular compartments within the papilla. Morgan (20) used inulin as a marker of extracellular space and calculated the composition and volume of all cell types in slices of rat papilla from his measurements. Neither of these techniques permitted exchange processes to be rapidly arrested before analysis.

In the present studies, kidneys were rapidly removed from anesthetized rats with as little surgery as possible, and wedge-shaped pieces containing papillae were frozen within a few seconds of kidney removal. The shock-freezing technique was used to eliminate chemical fixation, to minimize diffusion to maintain elemental localization, and to minimize ice-crystal size. Because the papilla was frozen whole, freezing was necessarily slowed, and ice crystals as large as 1 μm were found in extracellular compartments. The size of analytical raster scans were adjusted accordingly, so that each analysis represented the mean composition of a region including many small crystallization artifacts.

Elemental weight fractions (R-values) measured in tissue compartments in both hydrated and dried sections in all animals demonstrated reproducible and characteristic elemental patterns (Table I and Fig. 3). Although weight fractions differed in these compartments, estimations of concentration required knowledge of water content in each compartment. The water content of the whole renal papilla has been estimated by drying studies to be 76–89% (4, 5, 13, 15, 18). The water content measured within intracellular compartments in this study was ~60%. This is a value comparable to that measured by other investigators in muscle and liver cells (24). The high water content observed in the whole papilla reflects the presence of a large extracellular compartment. In fact interstitial water was 77.4% of the mass of this compartment and luminal water content in collecting-duct lumina was even higher (82.8%). Using the measured water content, the elemental concentrations in millimoles per kilogram of wet tissue were calculated (Table II). Although the relationship between concentration and ionic activity of each element is not known, concentration and activity may change in parallel. Thus, the availability of a technique permitting the direct measurement of water content

TABLE II

Compartmental Water Fractions and Elemental Concentrations

Compartment	% Water	Na	P	S	Cl	K
COLLECTING-DUCT CELL	56.7 ± 5.6					
Dry wt, *mm/kg*		795 ± 293	581 ± 46	67 ± 15	765 ± 249	360 ± 125
Wet wt, *mm/kg*		344 ± 127	252 ± 20	29 ± 6	331 ± 108	156 ± 54
Wet wt, *g/kg*		7.9 ± 2.9	7.8 ± 0.6	0.9 ± 0.2	11.8 ± 3.8	6.1 ± 2.6
PAPILLARY EPITHELIAL CELL	59.5 ± 10.8					
Dry wt, *mm/kg*		708 ± 261	597 ± 133	93 ± 39	785 ± 196	348 ± 90
Wet wt, *mm/kg*		287 ± 106	242 ± 54	39 ± 16	318 ± 79	141 ± 36
Wet wt, *g/kg*		6.6 ± 2.4	7.5 ± 1.7	1.2 ± 0.5	11.3 ± 2.8	5.5 ± 1.4
INTERSTITIAL CELL	59.9 ± 6.5					
Dry wt, *mm/kg*		2,236 ± 483	361 ± 65	64 ± 15	1,805 ± 348	197 ± 40
Wet wt, *mm/kg*		898 ± 194	145 ± 26	26 ± 6	725 ± 140	79 ± 16
Wet wt, *g/kg*		20.7 ± 4.5	4.5 ± 0.2	0.8 ± 0.2	25.7 ± 5.0	3.1 ± 0.6
INTERSTITIUM	77.4 ± 2.3					
Dry wt, *mm/kg*		2,609 ± 526	172 ± 52	120 ± 40	1,966 ± 508	186 ± 35
Wet wt, *mm/kg*		590 ± 119	40 ± 15	27 ± 9	445 ± 115	42 ± 8
Wet wt, *g/kg*		13.6 ± 2.7	1.2 ± 0.4	0.9 ± 0.3	15.8 ± 4.1	1.6 ± 0.3

Percent water is expressed as the mean ± SD of measurements made in five animals. Elemental concentrations (mean ± SD) are based on dry weight fractions (Table I), water content, and calibration factors based on the analysis of standard solutions (Eqs. 3 and 4).

TABLE III

Significance of Differences among Means of Compartmental Element Concentrations and Water Fractions

Concentration units	Element	Collecting-duct vs. papillary epithelial cell	Papillary epithelial vs. interstitial cells	Interstitial cell vs. interstitium	Collecting-duct vs. interstitial cells	Collecting-duct cells vs. interstitium
		P	*P*	*P*	*P*	*P*
Dry wt, *mm/kg*	Na	NS	<.001	NS	<.001	<.001
	P	NS	<.01	<.001	<.001	<.001
	S	NS	NS	<.01	NS	NS
	Cl	NS	<.001	NS	<.01	<.01
	K	NS	<.01	NS	<.02	<.02
Wet wt, *mm/kg*	Na	NS	<.001	<.01	<.001	<.01
	P	NS	<.01	<.001	<.001	<.001
	S	NS	NS	NS	NS	NS
	Cl	NS	<.001	<.01	<.001	NS
	K	NS	<.01	<.001	<.02	NS
% Water		NS	NS	<.001	NS	<.001

The data were treated as independent samples, using a pooled estimate of common variance, ten degrees of freedom, and a two-tailed Student's *t* test. *NS*, not significant; NS level, $P > .05$.

in defined papillary cell types is of great potential value.

Several sources of variation may explain the scatter in the experimental data. The greatest differences were found between observations made in different animals. The range of overnight urine osmolality in these animals was from 1,267 to 2,221 mosmol/liter. To shorten the surgical procedure, ureteral urine was not collected at nephrectomy. Because papillary composition has been shown to be extremely labile (2), collection of ureteral urine at the time of nephrectomy will be necessary for future physiological studies. The finding of closed collecting-duct lumina, although not typical of micropuncture preparations, may reflect a normal condition. In hamsters studied without opening the renal pelvis, collecting-duct flow has been found to be pulsatile (26). Within single tissue sections, different examples of the same morphological compartment occasionally differed markedly in elemental composition, although the standard deviations of means were usually ~20% of mean values. In the presence of these sources of variation, the variability introduced by counting statistics was small and was ignored in calculations. This was in contrast to the study of pure standards (22) in which specimen-to-specimen variation was small.

The measurements of interstitial fluid obtained in the present study appear consistent with measurements obtained by micropuncture, taking into account differences in urine concentration. For example, Battilana et al. (7) have measured the Na and K concentration in vasa recta plasma (probably reflecting interstitium) in rats whose collecting-duct osmolality was 938 mosmol/kg H_2O, approximately half of that of the urine of the rats in the present study. Assuming that interstitial concentration increased proportionally to urine concentration, then it might be expected that our concentrations would be twice as high. Battilana et al. (7) found a K of 36 ± 2 meq/kg H_2O, whereas we found 42 ± 8 mm/kg wet weight (54 mm/kg H_2O

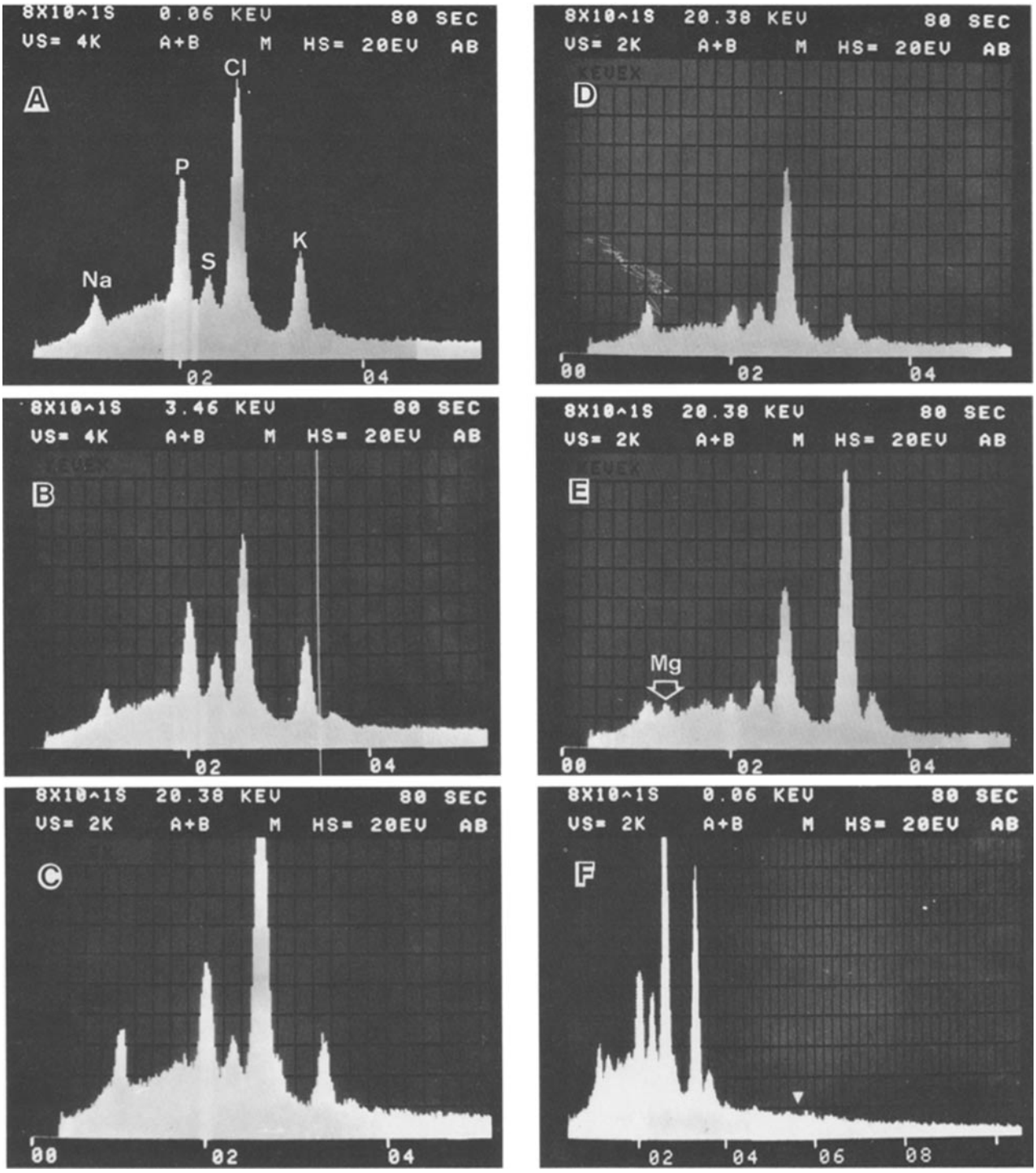

FIGURE 3 X-ray spectra obtained during microanalysis of defined compartments. In each spectrum, counting rate is displayed (vertical scale) as a function of x-ray energy in kiloelectronvolts (horizontal scale). Elemental peaks are identified. Because of differential excitation and absorption of different characteristic x-rays, it is not possible to relate peak height of different elements in spectra directly to relative concentration. *A*, cytoplasm of collecting-duct cell; *B*, cytoplasm of papillary epithelial cell; *C*, cytoplasm of interstitial cell; *D*, interstitial space; *E*, lumen of collecting duct; *F*, plasma in lumen of capillary vessel. In *F*, an arrow shows the theoretical position of an iron peak. The absence of this peak indicates that little or no smearing or hemolysis occurred.

at 77% water fraction). Similarly, Na concentration obtained by vascular micropuncture was 304 ± 12 meq/kg H_2O, whereas we measured 570 ± 119 mm/kg wet weight (766 mm/kg H_2O at 77% water fraction).

The similarity between the elemental content of collecting-duct and papillary epithelial cells was expected. Bonventre et al. (8) have shown that these cell types have ultrastructural similarities and that both respond to antidiuretic stimuli. These cells, and the interstitial cells, have higher sodium and chlorine content than other (nonrenal) cells as measured by x-ray microanalysis (11, 27, 28). Both Schmidt-Nielsen (25) and Morgan (20) have shown high intracellular sodium, but not potassium, concentrations in the renal papilla, and these findings are confirmed by the present study. The role of sodium

uptake in the mechanism of osmotic adaption is strengthened by the findings of Morgan (20) and Somlyo et al. (27) that cell sodium and chlorine increase when cells are immersed in hypertonic sodium chloride. The present study shows even higher intracellular sodium levels than reported by either Schmidt-Nielsen or Morgan. This may be because x-ray microanalysis measures both free and bound elements. Thus, it is too early to conclude that the high interstitial cell sodium indicates an active uptake process.

The authors wish to thank Mr. William Riley for his expert technical assistance.

This project was supported by National Institutes of Health (NIH) grants AM 26134, GM 15904, and AM 18249. Dr. Beeuwkes is the recipient of NIH RCDA AM 00224 and a grant from R. J. Reynolds Industries, Inc.

This study was presented in part as an abstract at the American Society of Nephrology meeting in Boston, Massachusetts, in November 1979.

Received for publication 3 December 1979, and in revised form 21 July 1980.

REFERENCES

1. Appelboom, J. W., W. A. Brodsky, and W. N. Scott. 1965. Effect of osmotic diuresis on intrarenal solutes in diabetes insipidus and hydropenia. *Am. J. Physiol.* 208:38–45.
2. Atherton, J. C. 1978. Lability of renal papillary tissue composition in the rat. *J. Physiol. (Lond.).* 274:323–328.
3. Atherton, J. C., J. A. Evens, R. Green, and S. Thomas. 1971. Influence of variations in hydration and in solute excretion on the effects of lysine-vasopressin infusion on urinary and renal tissue composition in the conscious rat. *J. Physiol. (Lond.).* 213:311–327.
4. Atherton, J. C., R. Green, and S. Thomas. 1971. Influence of lysine-vasopressin dosage on the time course of changes in renal tissue and urinary composition in the conscious rat. *J. Physiol. (Lond.).* 213:291–309.
5. Atherton, J. C., M. A. Hai, and S. Thomas. 1968. The time course of changes in renal tissue composition during mannitol diuresis in the rat. *J. Physiol. (Lond.).* 197:411–428.
6. Atherton, J. C., M. A. Hai, and S. Thomas. 1968. The time course of changes in renal tissue composition during water diuresis in the rat. *J. Physiol. (Lond.).* 197:429–443.
7. Battilana, C. A., D. C. Dobyan, F. B. Lacy, J. Bhattacharya, P. A. Johnston, and R. L. Jamison. 1978. Effect of chronic potassium loading on potassium secretion by the pars recta or descending limb of the juxtamedullary nephron in the rat. *J. Clin. Invest.* 62: 1093–1103.
8. Bonventre, J. V., M. J. Karnovsky, and C. P. Lechene. 1978. Renal papillary epithelial morphology in antidiuresis and water diuresis. *Am. J. Physiol.* 235:F69–F76.
9. Bulger, R. E., and R. B. Nagle. 1973. Ultrastructure of the interstitium in the rabbit kidney. *Am. J. Anat.* 136:183–204.
10. Bulger, R. E., and B. F. Trump. 1966. Fine structure of the rat renal papilla. *Am. J. Anat.* 118:685–722.
11. Cameron, I. L., N. K. R. Smith, and T. B. Pool. 1979. Element concentration changes in mitotically active and postmitotic enterocytes. An x-ray microanalysis study. *J. Cell Biol.* 80:444–450.
12. Cross, R. B. 1964. The effects of osmotic diuresis and vasopressin upon the distribution of sodium, potassium and urea in the rat kidney. *Aust. J. Exp. Biol. Med. Sci.* 42:523–538.
13. Gardner, K. D., and J. M. Vierling. 1969. Solids, water, and solutes in papillary region of the rat kidney. *Am. J. Physiol.* 217:58–64.
14. Gottschalk, C. W., and M. Mulle. 1959. Micropuncturestudy of the mammalian urinary concentrating mechanism: evidence for the countercurrent hypothesis. *Am. J. Physiol.* 196: 927–936.
15. Hai, M. A., and S. Thomas. 1969. The time-course of changes in renal tissue composition during lysine vasopressin infusion in the rat. *Pfluegers Arch. Eur. J. Physiol.* 310:297–319.
16. Hall, T. A., H. C. Anderson, and T. Appleton. 1973. The use of thin specimens for x-ray microanalysis in biology. *J. Microsc. (Oxf.).* 99:177–182.
17. Jamison, R. L. 1968. Micropuncture study of segments of thin loops of Henle in the rat. *Am. J. Physiol.* 215:126–141.
18. Levitin, H., A. Goodman, G. Pigeon, and F. H. Epstein. 1962. Composition of the renal medulla during water diuresis. *J. Clin. Invest.* 41:1145–1151.
19. Moreton, R. B., P. Echlin, B. L. Gupta, T. A. Hall, and T. Weis-Fogh. 1974. Preparation of frozen hydrated tissue sections for x-ray microanalysis in the scanning electron microscope. *Nature (Lond.).* 247:113–115.
20. Morgan, T. 1977. Effect of NaCl on composition and volume of cells of the rat papilla. *Am. J. Physiol.* 232:F117–F122.
21. Saikia, T. C. 1965. Composition of the renal cortex and medulla of rats during water diuresis and antidiuresis. *Q. J. Exp. Physiol. Congn. Med. Sci.* 50:146–157.
22. Saubermann, A. J., R. Beeuwkes III, and P. D. Peters. 1981. Application of scanning electron microscopy to x-ray analysis of frozen-hydrated sections. II. Analysis of standard solutions and artificial electrolyte gradients. *J. Cell Biol.* 88:268–273.
23. Saubermann, A. J., P. Echlin, P. D. Peters, and R. Beeuwkes III. 1981. Application of scanning electron microscopy to x-ray analysis of frozen-hydrated sections. I. Specimen handling techniques. *J. Cell Biol.* 88:257–267.
24. Saubermann, A. J., W. D. Riley, and P. Echlin. 1977. Preparation of frozen hydrated tissue sections for x-ray microanalysis using a satellite vacuum coating and transfer system. *Scanning Electron Microsc.* 1:347–356.
25. Schmidt-Nielsen, B. 1975. Comparative physiology of cellular ion and volume regulation. *J. Exp. Zool.* 194:207–220.
26. Schmidt-Nielsen, B., and L. N. Reinking. 1979. Pulsatile movement of urine through the papillary collecting ducts in hamsters. *In* Abstracts of the 12th Annual Meeting, American Society of Nephrology, Boston, Mass. 60A.
27. Somlyo, A. V., H. Shuman, and A. P. Somlyo. 1977. Elemental distribution in striated muscle and the effects of hypertonicity. Electron probe analysis of cryosections. *J. Cell Biol.* 74:828–857.
28. Somlyo, A. P., A. V. Somlyo, and H. Shuman. 1979. Electron probe analysis of vascular smooth muscle. *J. Cell Biol.* 81:316–335.
29. Wirz, V. H. 1953. Der osmotische Druck des Blutes in der Nierenpapille. *Helv. Physiol. Pharmacol. Acta.* 11:20–29.
30. Wirz, V. H., B. Hargitay, and W. Kuhn. 1951. Lokalisation des Konzentrierungsprozesses in der Niere durch direkte Kryoskopie. *Helv. Physiol. Pharmacol. Acta.* 9:196–207.